

# The histology and function of the dermal armour of the aetosaur *Stagonolepis olenkae* Sulej, 2010 (Archosauria, Pseudosuchia) from Krasiejów (SW Poland)

PRZEMYSŁAW BŁASZCZEĆ<sup>1</sup> and MATEUSZ ANTCZAK<sup>2</sup>

<sup>1</sup> Institute of Geology, Adam Mickiewicz University, Krygowskiego 12, 61-680 Poznań, Poland; email: przbla1@amu.edu.pl

<sup>2</sup> Institute of Biology, University of Opole, Oleska 22, 45-052 Opole, Poland; email: mateusz.antczak@uni.opole.pl

## ABSTRACT:

Błaszczec, P. and Antczak, M. 2025. The histology and function of the dermal armour of the aetosaur *Stagonolepis olenkae* Sulej, 2010 (Archosauria, Pseudosuchia) from Krasiejów (SW Poland). *Acta Geologica Polonica*, 75 (1), e38.

Microscopic observations of the bone tissues of osteoderms covering an animal's body can provide an insight into its lifestyle and ontogeny as well as reveal the function of the armour. In the case of the aetosaur *Stagonolepis olenkae* Sulej, 2010 from the locality of Krasiejów, to date only the paramedian osteoderms have been analysed and compared to other taxa within Pseudosuchia Zittel, 1887. This study examines ten disarticulated plates from different parts of the body of *S. olenkae*: paramedian, lateral, ventral and appendicular osteoderms. The armour of *S. olenkae* has a diploe structure composed of layers of external and basal cortex surrounding an internal cancellous core. In the basal layer of the osteoderms, bundles of Sharpey's fibres and skeletochronological structures are present. The internal structures of the osteoderms indicate extensive remodelling processes, and the weak vascularization and bone tissues that constitute the plates – lamellar bone and parallel-fibred bone – suggest considerable mechanical resistance. Elements of the armour's osteology adapted to distribute and reduce mechanical stress might provide confirmation of the protective function of the armour as well.

**Key words:** Aetosauria; *Stagonolepis*; Osteoderms; Palaeohistology.

## INTRODUCTION

Osteoderms are mineralized structures formed within the dermis, usually in the form of bony plates of various shapes, sizes and ornamentation (Vickaryous and Hall 2008). They can function as mechanical protection (Broeckhoven *et al.* 2015), reduce the buoyancy of aquatic organisms (Houssaye 2009), assist in thermal regulation of ectothermic organisms, participate in lactic acid buffering in hypoxic conditions (Clarac *et al.* 2018), store calcium in reproductively active females (Dacke *et al.* 2015), or fulfil several functions at the same time

(Seidel 1979; Nasoori 2020). Histological analysis of tissues that constitute them allows their function to be determined (Broeckhoven *et al.* 2017; du Plessis *et al.* 2018; Clarac *et al.* 2019; Pochat-Cottilloux *et al.* 2022).

Aetosaurs (Archosauria: Pseudosuchia) were a group of armoured quadrupedal medium- to large-sized (Small 1985; Heckert and Lucas 1999; Desojo *et al.* 2013) archosaurs (Nesbitt 2011). During the Late Triassic (Carnian to Rhaetian), they lived almost throughout Pangea, with fossils found in North and South America, Africa, Europe and India (Heckert and Lucas 1999; Desojo *et al.* 2013). Initially de-



scribed as herbivores, after analysis of the structure and mechanics of the skull and the forelimbs (Small 2002; Desojo and Vizcaíno 2009; Sulej 2010; Drózd 2018; Taborda *et al.* 2021), they were recognised as omnivores who used their snout and strong limbs to excavate underground stems and insects (Sulej 2010; Antczak 2012). An extensive bony armour was a distinctive feature of aetosaurs, whose back and abdomen from the back of the head to the tip of the tail were covered by columns of often interlocking osteoderms. Occasionally, appendicular osteoderms also covered the limbs (Desojo *et al.* 2013; Parker 2016; Drózd 2018; UOPB collection, personal observations).

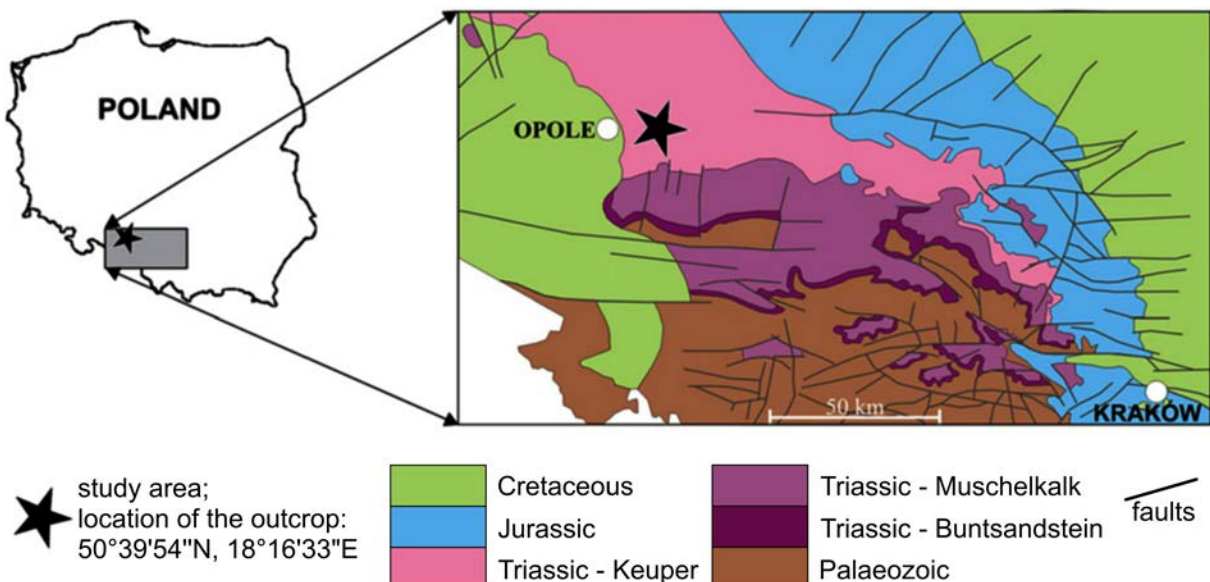
To date, the histology of aetosaur osteoderms has been studied several times, but with a primary focus on selected elements of the armour or comparing the microstructure of single osteoderms within Aetosauria or with other archosaurs. A more detailed description was performed twice – for the species *Aetosauroides scagliai* Casamiquela, 1960 (Cerdeja *et al.* 2018) and *Coahomasuchus chathamensis* Heckert, Fraser and Schneider, 2017 (Hoffman *et al.* 2018). In the case of *Stagonolepis olenkae*, a histological description was performed only for the paramedian osteoderms (Scheyer *et al.* 2014; Cerdeja *et al.* 2018), but a detailed characterization of the bone tissues of the entire armour of this aetosaur has never been provided. Additionally, a description of the tissues constituting the osteoderms of *S. olenkae* will provide insight into the possible function of the dermal armour. It is theorized that the dermal armour of aetosaurs provided a protection against predators (Dzik

and Sulej 2007; Drózd 2018; Keeble and Benton 2020), but this has not yet been confirmed by more thorough analyses (Drymala *et al.* 2021).

## GEOLOGICAL SETTING

Krasiejów is a village located in Opole Voivodeship (Upper Silesia, SW Poland) and situated geologically on the south-eastern edge of the Fore-Sudetic Homocline (Text-fig. 1). The abandoned post-mining clay pit is an outcrop of Upper Triassic fine-grained sedimentary rocks: siltstones, mudstones and claystones, with less frequent sandstones and calcareous nodules (Bodzioch and Kowal-Linka 2012; Szulc and Racki 2015; Szulc *et al.* 2015a, b).

Within the site, three units have been distinguished, consisting of two, upper and lower, bone-bearing beds (Gruszka and Zieliński 2008; Bodzioch and Kowal-Linka 2012; Szulc and Racki 2015; Szulc *et al.* 2015b). Aetosaur bones and osteoderms can be found in this section of the outcrop. The lower bonebed is the richest, an accumulation of mostly disarticulated remains of Temnospondyli (such as *Metoposaurus* Lydekker, 1890 and *Cyclotosaurus* Fraas, 1889); the pseudosuchian archosaurs *Parasuchus* Lydekker, 1885 (Phytosauria), *Stagonolepis* Agassiz, 1844 (Aetosauria), *Polonosuchus* Brusatte, Butler, Sulej and Niedźwiedzki, 2009 (Rauisuchia), and the avemetatarsalian archosaur *Silesaurus* Dzik, 2003 (Dinosauriformes?) (Dzik *et al.* 2000; Sulej and Majer 2005; Dzik and Sulej 2007; Brusatte *et al.*



Text-fig. 1. Geological setting of the study area (after Bodzioch and Kowal-Linka 2012).



*ertsoni* may be explained by ontogeny or sexual dimorphism; *S. olenkae* could also represent a local variation (Antczak 2016a).

*Stagonolepis olenkae* is one of the largest archosaurs found in the Krasiejów deposits – it is second in size only to the raiusuchian *Polonosuchus silesiacus* Brusatte, Butler, Sulej and Niedźwiedzki, 2009 (Sulej 2005). The aetosaur's armour may have provided a form of defence against attacks by predators such as the raiusuchian *P. silesiacus* (Dzik and Sulej 2007; Sulej 2010).

The paramedian osteoderms of *Stagonolepis* are rectangular, with a width-to-length ratio of approximately 2.5:1 (Heckert and Lucas 2000; Parker 2018), distinctly ornamented, with a radial pattern of grooves and pits radiating from an eminence located at the posterior margin of the plate. The paramedian and ventral elements have an anterior bar overlapping the preceding plate in the column. The lateral osteoderms tend to be rectangular in shape and, depending on the row, may be flat or equipped with a pointed keel at the medial edge. Their angulation is more pronounced than that of the paramedian osteoderms. The appendicular osteoderms are rhomboidal (Parker 2003).

## MATERIALS AND METHODS

The material studied includes 10 osteoderms of the aetosaur *Stagonolepis olenkae* from different parts of the lower bonebed from Krasiejów and these were taken from the collection at Opole University (UOPB3645–3649, UOBS00148, 02174, 02258, 02395, 02876). Their position on the animal's body was determined based on their osteological features (as described by Parker 2003) (Text-fig. 3). For a complete insight into the microstructure of the armour, the paramedian, lateral, ventral and appendicular osteoderms

(Text-figs 4, 5) were analysed. All osteoderms were photographed and measured before sectioning.

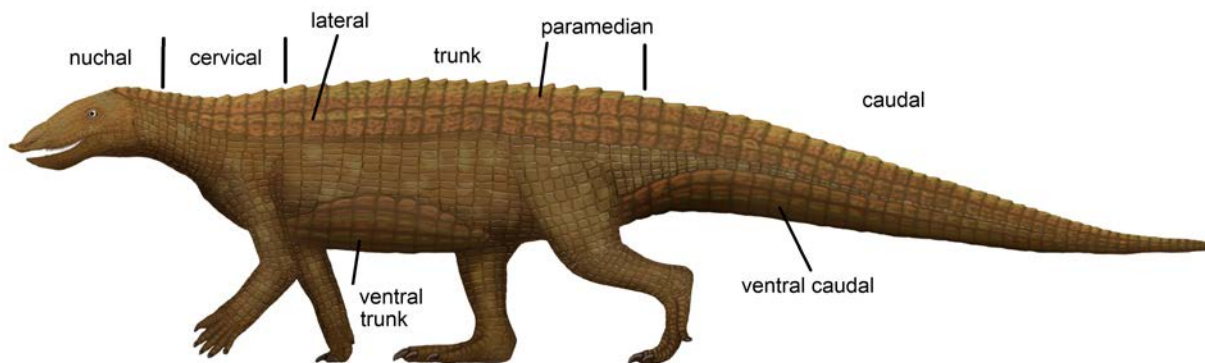
The osteoderms were prepared manually and chemically with the use of a 30% hydrogen peroxide solution. The thin sections were prepared at the Institute of Geology, Adam Mickiewicz University in Poznań, using the standard methods for the preparation of palaeohistological thin sections (Chinasamy and Raath 1992). Due to their high degree of brittleness, the osteoderms were coated with a layer of Araldite 2020 A and B two-component epoxy adhesive. Planned sections were made using a Struers Discoplan-TS laboratory saw and a WS 20A wire saw. The thin sections were then pre-sanded manually, using circular motions, with carborundum powders of 600 and 1200 grit. Any residual powder was removed by bathing in an ultrasonic cleaner. The prepared fragments were bonded to the glass slides using Araldite 2000 adhesive. The thin sections were ground with a Logitech PM5 grinder to a thickness of 60–80 µm and then manually polished with a 1200 grit carborundum powder again. Data on osteoderm location (paramedian, lateral, ventral, appendicular), and the measurements and planes of sectioning are compiled in Table 1.

Microscope observations (Text-fig. 6) were carried out under transmitted ordinary and polarized light using a Leica M205 C stereo microscope with a polarization filter attachment and Leica LAS software.

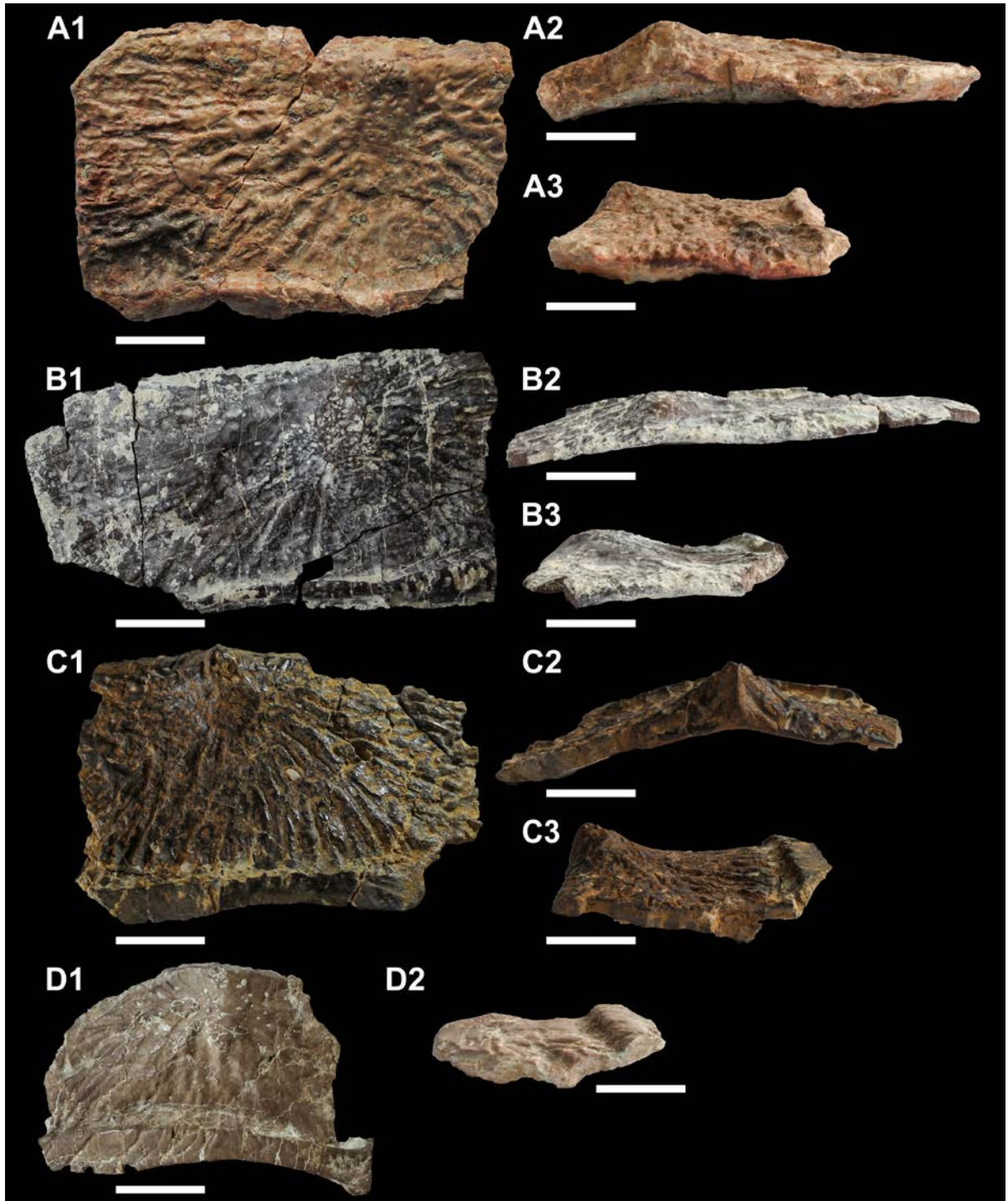
## OBSERVATIONS

**Paramedian osteoderms** (UOPB3645, UOPB3646, UOBS02876, UOBS02258)

*External cortex.* The external cortex is composed of a lamellar bone or parallel-fibred bone of a variable thickness which ranges from 0.7–1 mm for pits and grooves to about 1–2.5 mm for ridges, depending



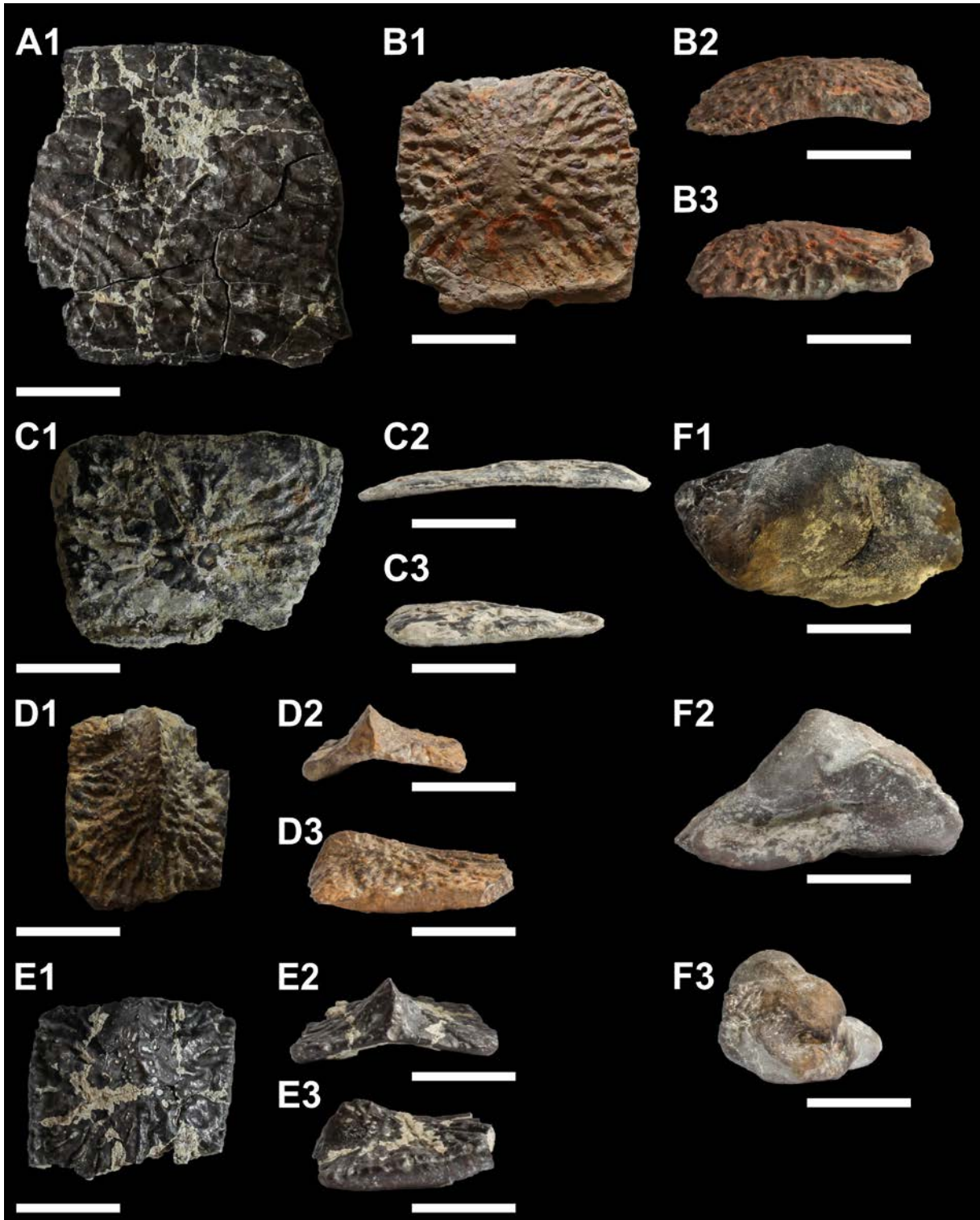
Text-fig. 3. *Stagonolepis* reconstruction and explanation of osteoderm division based on the location in the body (after Parker 2016; reconstruction of *Stagonolepis* drawn by S. Górnicki).



Text-fig. 4. Paramedian osteoderms UOPB3645 (A), UOPB3646 (B), UOBS02876 (C) and UOBS02258 (D) of *Stagonolepis olenkae* Sulej, 2010 in external view with anterior bar edge located towards the bottom of the picture (A1, B1, C1, D1); posterior edge view (A2, B2, C2); osteoderms in lateral view with anterior bar edge located towards the right margin of the picture (A3, B3, C3, D2). Scale bar equals to 20 mm.

on the ornamentation feature. Evidence of intensive bone resorption and deposition processes (Text-figs 7A, B, 8D, 9F, rl) is present, especially around the or-

nammentation structures and anterior bar. The cortex is vascularized primarily by vascular canals, primary osteons and scattered secondary osteons (Text-figs



Text-fig. 5. Ventral UOBS00148 (A), UOBS02395 (B) UOBS02174 (C), lateral UOPB3647 (D), UOPB3649 (E) and appendicular UOPB3648 (F) osteoderms of *Stagonolepis olenkae* Sulej, 2010. Ventral elements: external view with anterior bar located towards the bottom of the picture (A1, B1, C1); posterior edge view of ventral osteoderms (B2, C2); lateral view with anterior bar located towards the right margin of the picture (B3, C3). Lateral osteoderms: external view with anterior edge located towards the bottom of the picture (D1, E1); posterior edge view (D2, E2); lateral view with anterior edge located towards the right margin of the picture (D3, E3). Appendicular osteoderm: external view (F1); posterior edge view (F2), lateral view (F3). Scale bar equals to 20 mm.

Specimen no.	Element	Width [cm]	Length [cm]	Plane of sectioning
UOPB3645 (Text-fig. 4A1–A3)	large, thick paramedian osteoderm fragment with damaged anterior bar	9.8	6.7	parasagittal, transversal
UOPB3646 (Text-fig. 4B1–B3)	paramedian osteoderm fragment with less prominent ornamentation and damaged dorsal eminence	10.5	5.9	parasagittal, transversal
UOBS02876 (Text-fig. 4C1–C3)	paramedian osteoderm fragment with prominent ornamentation and well-preserved dorsal eminence (knob) and anterior bar	9.0	6.2	parasagittal, transversal
UOBS02258 (Text-fig. 4D1–D2)	paramedian osteoderm fragment with less prominent ornamentation and well-preserved anteromedial process	7.4	5.2	parasagittal
UOBS00148 (Text-fig. 5A1)	flat, thin ventral osteoderm fragment	6.2	6.2	–
UOBS02395 (Text-fig. 5B1–B3)	flat, square-shaped ventral osteoderm with prominent ornamentation	4.7	4.7	–
UOBS02174 (Text-fig. 5C1–C3)	flat, trapezoidal ventral osteoderm	5.6	4.2	parasagittal
UOPB3647 (Text-fig. 5D1–D3)	keeled lateral osteoderm	3.1	3.9	parasagittal
UOPB3649 (Text-fig. 5E1–E3)	keeled lateral osteoderm	4.0	3.5	–
UOPB3648 (Text-fig. 5F1–F3)	rhomboidal appendicular osteoderm without ornamentation	5.5	3.1	oblique

Table 1. List of specimens used in the study.

7A, B, 8C, 9E). Specimen UOBS02258 shows a structure resembling a drifting secondary osteon (Robling and Stout 1999) – a radially arranged secondary osteon that changed its position towards the core of the osteoderm during growth. The secondary osteon possibly opened up onto the dorsal bone surface within an ornamentation valley just above the structure. The valley was filled with a compact cortex of the later growth stages, leading to an ornamentation pattern shift during ontogeny (Text-fig. 8D).

*Internal core.* The internal core is formed by an extensive structure of trabeculae composed of the lamellar bone (Text-figs 7C–E, 8A, 9A). The thicker trabeculae show the sporadic trabecular osteons with a diameter reaching 500  $\mu\text{m}$ , and the total thickness of the concentric lamellae reaches 130  $\mu\text{m}$ .

*Basal cortex.* The basal cortex is formed by either a lamellar-zonal bone composed of parallel-fibred bone with a varying degree of collagen fibre organisation (UOBS02258) or parallel-fibred bone with growth marks. The collagen fibres are mostly parallel to the cross-sectional plane of the thin section and form bright stripes under polarized light (Text-figs 7E, 8B, F, 9A, D, 10A). The basal cortex is sparsely vascularized by scattered irregular vascular channels parallel to the longer axis of the osteoderm forming elongated channels (Text-fig. 7F) or small concentrations thereof; their count decreases towards the periosteum. The exception is specimen UOBS02258, which has the most vascularized basal layer of all four paramedian osteoderms analysed. In addition, Sharpey's fibres are also found forming dense and tightly packed coarse bundles (Text-figs 7F, 10B: ShF). The basal cortex of the paramedian

osteoderms can reach a thickness of 1 to 3 mm. One thin section of specimen UOBS02876 shows an area where its basal cortex is thinnest, reaching about 0.5 mm (Text-fig. 9C). Skeletochronological structures are also visible: 6 to 8 alternating zones of rapid and decreased bone growth can be traced (Text-fig. 9B), which is most prominent near the posterior edges of the osteoderms. Two cycles of bone growth can be seen in specimen UOBS02258, formed as zones of a sparsely organised parallel-fibred bone (isotropic under polarized light and characterised by round lacunae), and wide annuli from a parallel-fibred bone with a higher degree of organisation: anisotropic, with flattened and elongated lacunae aligned to the direction of collagen fibres (Text-fig. 8B, F). Both cycles are separated by rest lines (Text-fig. 8E, F). In addition, rusty-red iron oxide accumulations – pseudomorphing pyrite – are present in the trabeculae and fractures of one of the osteoderms analysed.

#### Lateral osteoderm (UOPB3647, UOPB3649)

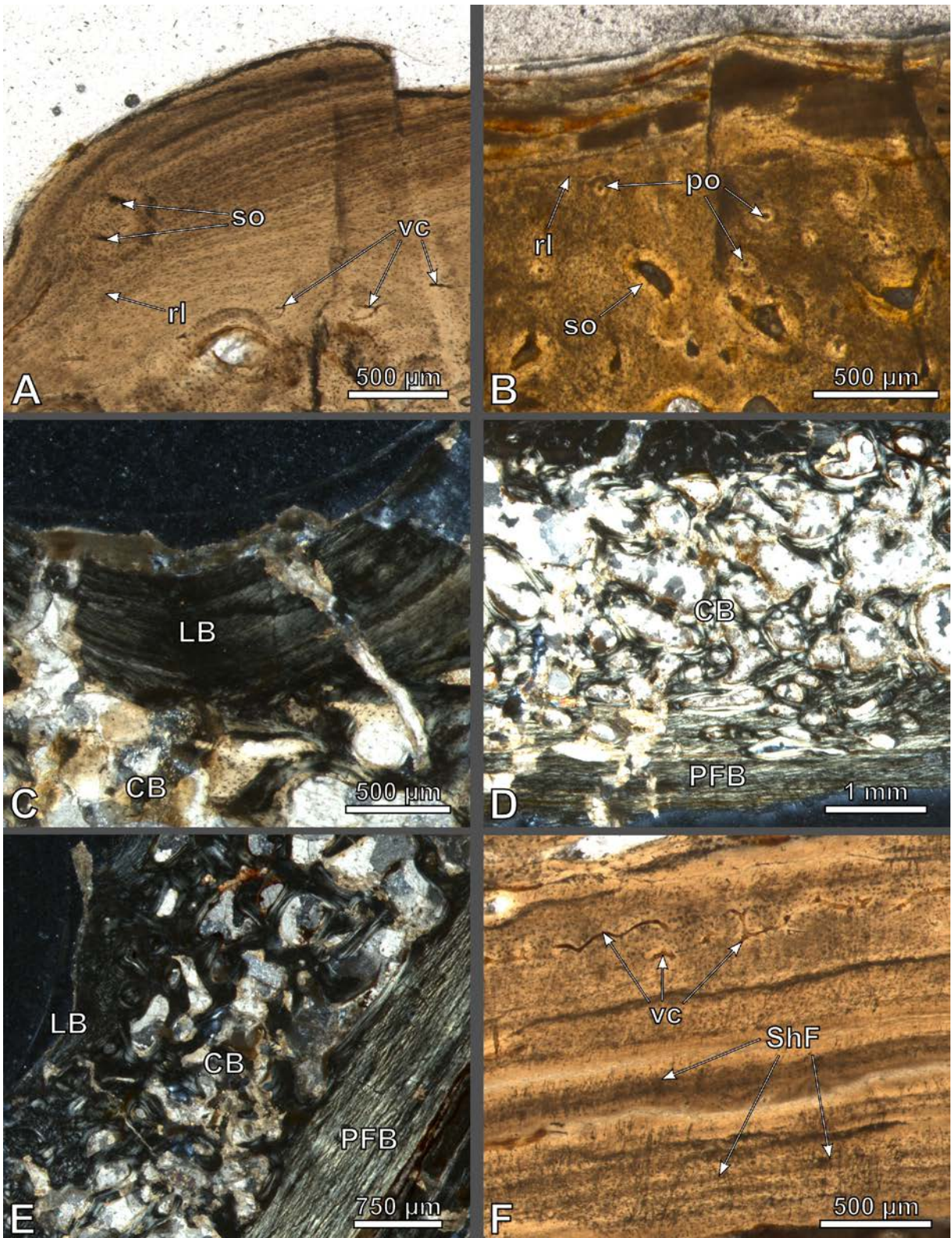
*External cortex.* The areas of bone remodelling the external cortex are composed of a lamellar bone or parallel-fibred bone (especially in the keeled region) with collagen fibres finer than those of the analogous tissue of the basal cortex. Its thickness reaches approximately 1 mm. The external cortex is mostly vascularized by simple vascular channels (most abundant in the anterior part of the osteoderm), secondary osteons and sparse primary osteons. The keeled region shows erosion cavities exceeding 2 mm in length and extending to the internal core of the specimen (Text-fig. 10C).



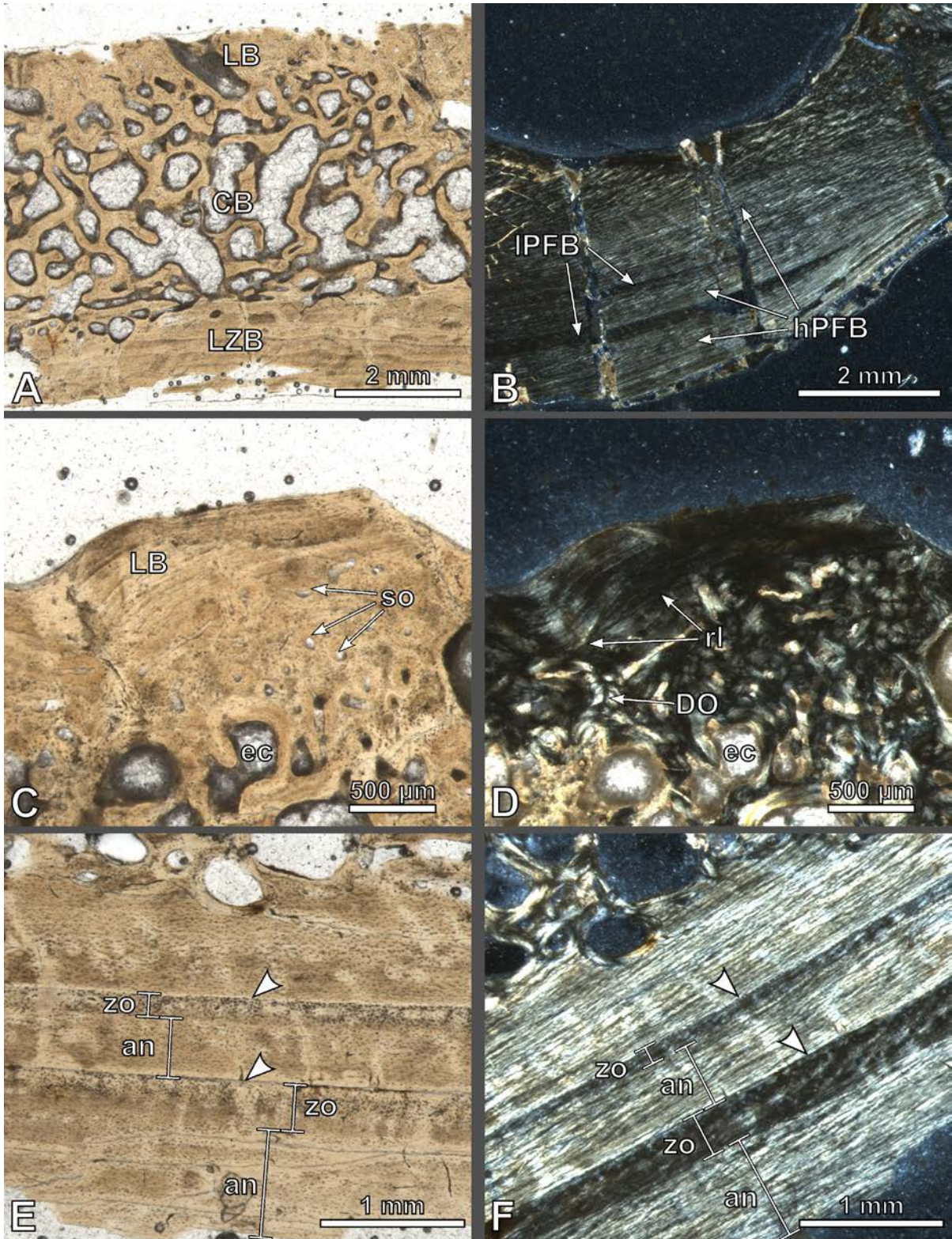
Text-fig. 6. Osteoderm microstructure of *Stagonolepis olenkae* Sulej, 2010: paramedian UOPB3645 (A), UOPB3646 (B), UOBS02876 (C), UOBS02258 (D), ventral UOBS02174 (E), lateral UOPB3647 (F), and appendicular UOPB3648 (G) elements. Scale bar equals to 10 mm.

*Internal core.* The cancellous bone of the internal core is composed of thick trabeculae and present almost throughout the entire thin section: mostly in the

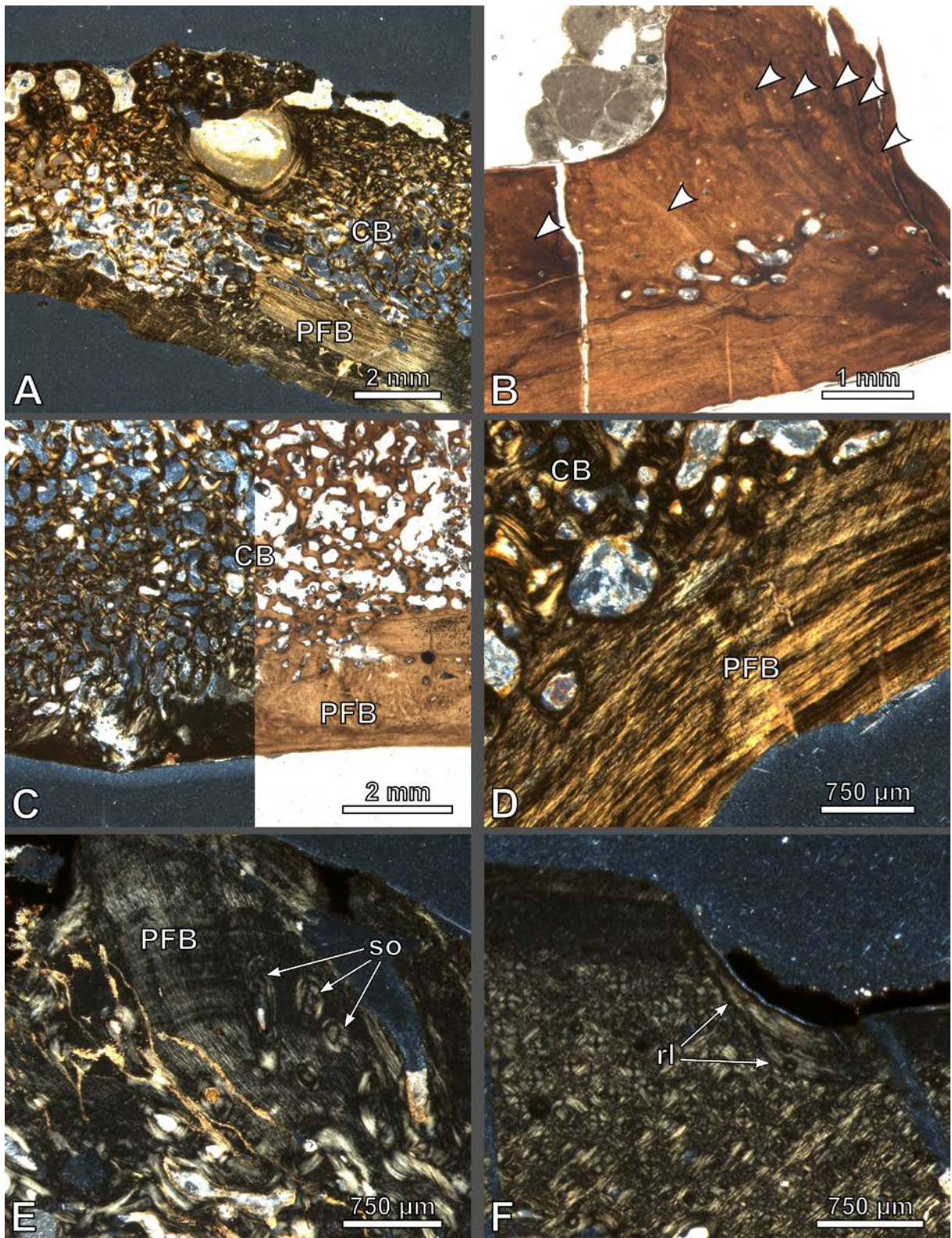
posterior part of the osteoderm and in the keel region. Towards the anterior margin of the osteoderm, the cancellous bone is minimal and gradually disappears.



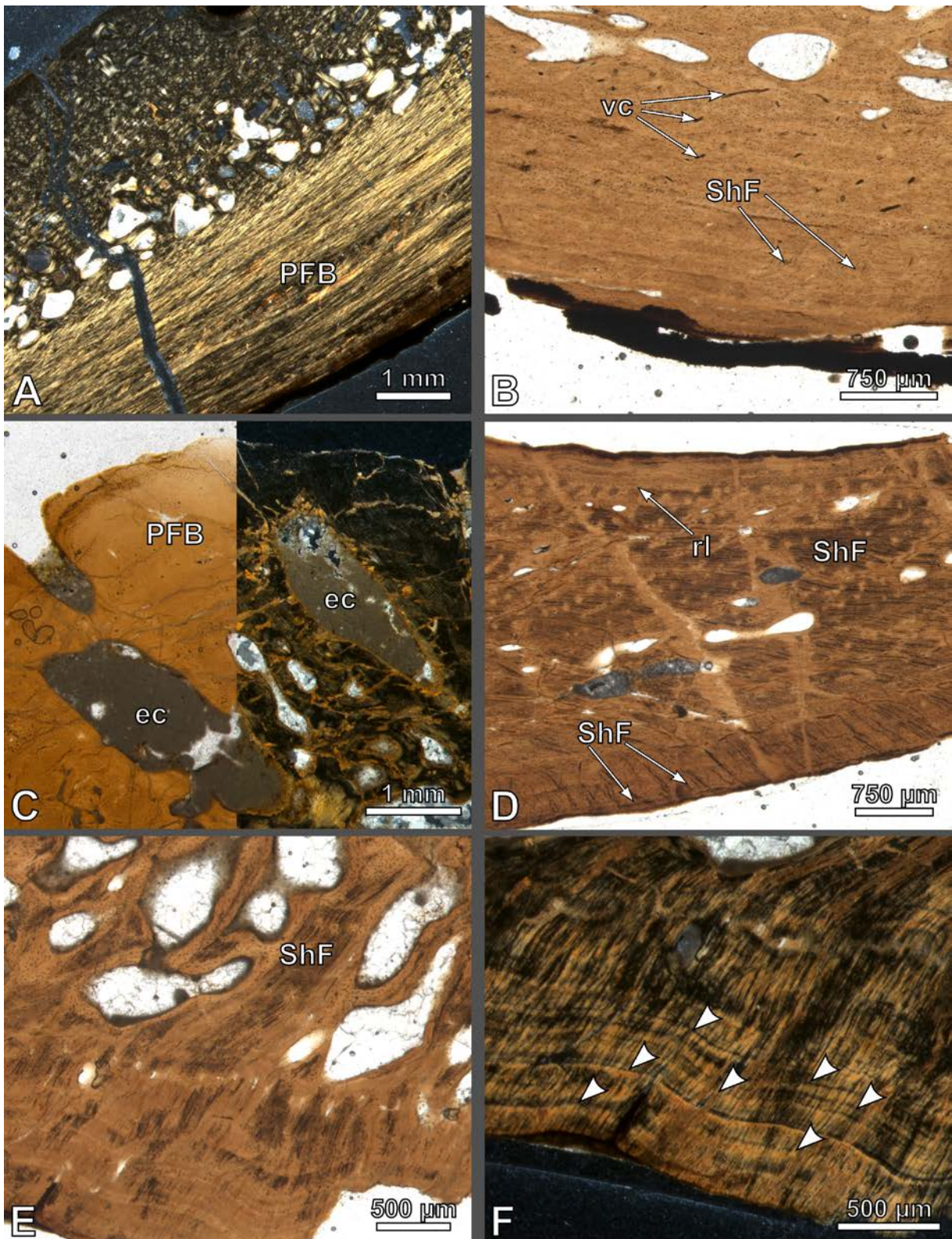
Text-fig. 7. *Stagonolepis olenkae* Sulej, 2010 paramedian UOPB3645 osteoderm histology. A, B, F – ordinary light; C, D, E – polarized light. Abbreviations: CB – cancellous bone; LB – lamellar bone; PFB – parallel-fibred bone; po – primary osteons; rl – resorption line; ShF – Sharpey's fibres; so – secondary osteons, vc – vascular canals.



Text-fig. 8. *Stagonolepis olenkae* Sulej, 2010 paramedian UOBS02258 osteoderm histology. A, C, E – ordinary light; B, D, F – polarized light. The arrows indicate the rest lines. Abbreviations: an – annulus; CB – cancellous bone; DO – drifting osteon; ec – erosion cavities; hPFB – parallel-fibred bone with a high degree of organisation; IPFB – parallel-fibred bone with a low degree of organisation; LB – lamellar bone; LZB – lamellar-zonal bone; rl – resorption line; so – secondary osteons; zo – zones.



Text-fig. 9. *Stagonolepis olenkae* Sulej, 2010 paramedian UOPB3646, UOBS02876 osteoderm histology. A, D, E, F – polarized light; B – ordinary light; C – polarized and ordinary light. Arrows indicate the start of subsequent cycles of bone growth. Abbreviations: CB – cancellous bone; PFB – parallel-fibred bone; rl – resorption line; so – secondary osteons.



Text-fig. 10. *Stagonolepis olenkae* Sulej, 2010 paramedian UOBS02876 (A, B) and lateral UOPB3647 (C–F) osteoderm histology. A, D, F – polarized light; B, E – ordinary light; C – ordinary and polarized light. Arrows indicate the start of subsequent cycles of bone growth. Abbreviations: ec – erosion cavity; PFB – parallel-fibred bone; rl – resorption line; ShF – Sharpey’s fibres; vc – vascular canals.

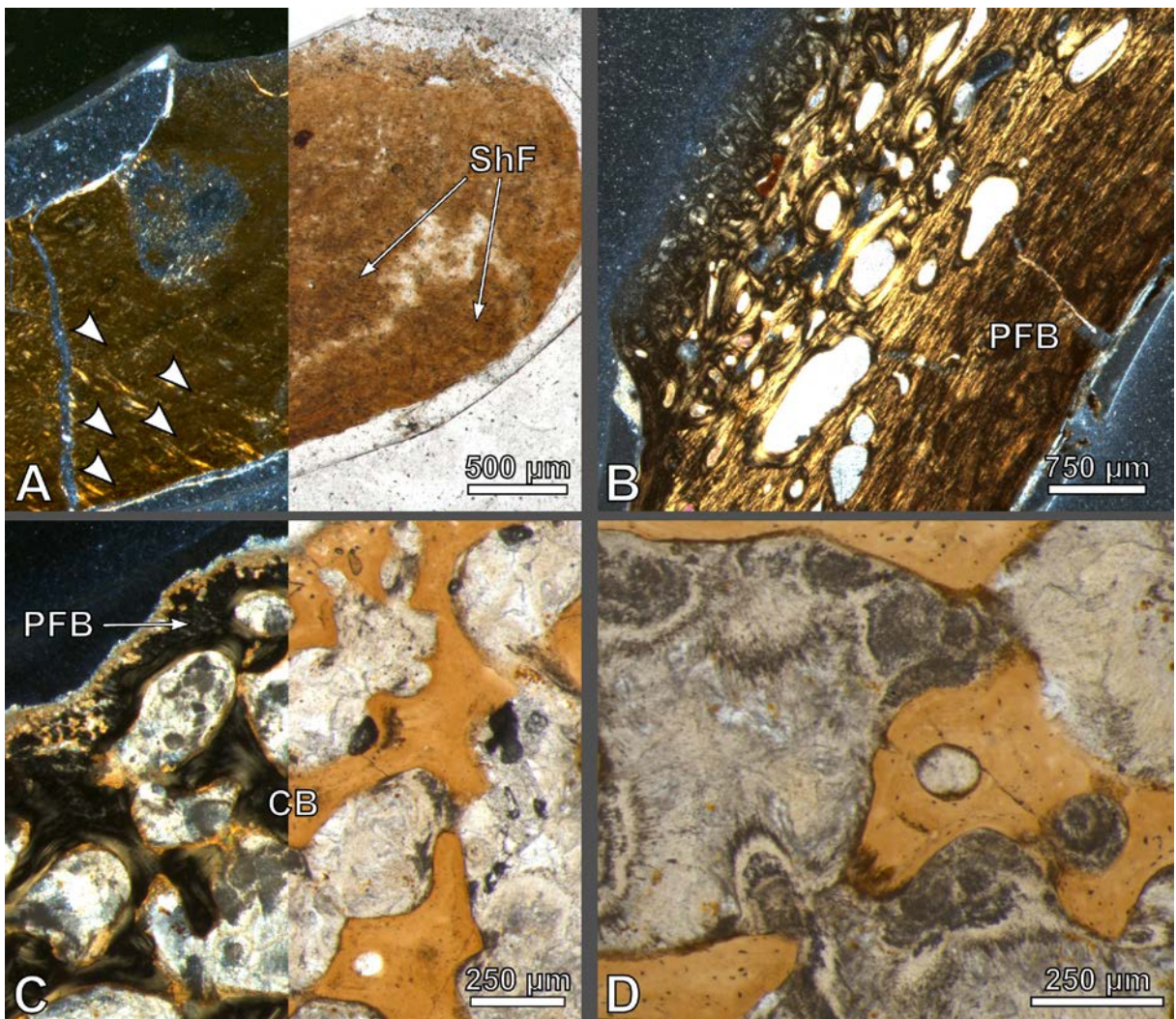
In the anterior part of the specimen, the only structures of secondary bone remodelling are secondary osteons (often with very thick lamellae – with a total thickness reaching 130  $\mu\text{m}$ ) and erosion cavities. The trabeculae consist of lamellar bone and reach a thickness of up to 300  $\mu\text{m}$ . Sparse trabecular osteons are also present.

**Basal cortex.** The basal cortex is composed of parallel-fibred bone with growth marks. Coarse bundles of Sharpey's fibres are abundant and occur along the entire length of the basal layer. The Sharpey's fibres insert at a moderate angle of  $40^\circ$  into the cortex and reach a thickness of up to 8  $\mu\text{m}$  (Text-fig. 10D, ShF). Numerous similar collagen structures with a single orientation can be also observed and their high density resembles Sharpey's fibre bone as described by Vickaryous and Hall (2006). These thick fibres

form massive bundles and are parallel to the surface of the osteoderm and sometimes extend to the cancellous core (Text-fig. 10D, E). Skeletochronologic structures are also traceable (a minimum of seven growth cycles; Text-fig. 10F).

**Ventral osteoderm** (UOBS00148, UOBS02174, UOBS02395)

**External cortex.** The external cortex is composed of a lamellar bone with traces of bone erosion and deposition in the regions of the surface ornamentation and at the anterior bar. The cortex is vascularized by primary and secondary osteons occurring mostly in clusters, especially around the ornamentation ridges (Text-fig. 11B). These clusters resemble



Text-fig. 11. *Stagonolepis olenkae* Sulej, 2010 ventral UOBS02174 (A, B) and appendicular UOPB3648 (C, D) osteoderm histology. A, C – polarized and ordinary light; B – polarized light; D – ordinary light. Arrows indicate the start of subsequent cycles of bone growth. Abbreviations: CB – cancellous bone; PFB – parallel-fibred bone; ShF – Sharpey's fibres.

the Haversian substitutional front (*sensu* Mitchell and Sander 2014), extending from the internal region to the external cortex of the osteoderm.

*Internal core.* The trabeculae are absent, and the only structures of secondary bone remodelling present are secondary osteons and erosion cavities, often of considerable size – reaching up to 1 mm in length and 0.4 mm in width (Text-fig. 11B).

*Basal cortex.* The basal cortex is composed of a weakly vascularized parallel-fibred bone reaching a thickness up to 0.8 mm. Approximately five growth cycles separated by rest lines can be traced in the basal layer. Sharpey's fibres are also present, including in the area of the osteoderm margin, although these are not as dense as in the paramedian or lateral osteoderms (Text-fig. 11A).

### Appendicular osteoderm (UOPB3648)

*External cortex.* The external cortex of the appendicular osteoderm is the thinnest of all the osteoderms studied, reaching a thickness of up to c. 0.3 mm, which is the result of extensive bone remodelling. The external cortex consists of a parallel-fibred bone with a low degree of organisation and devoid of growth marks. Lacunae are round and chaotically arranged (Text-fig. 11C). Due to the structural arrangement, skeletochronological structures are absent. The basal cortex is composed of the same tissue and structures.

*Internal core.* The cancellous interior consists of a well-developed network of secondary trabeculae composed of a lamellar bone and arranged concentrically. The trabeculae occupy a significant volume of the osteoderm and show signs of bone remodelling in the form of resorption lines; sparse osteons are also present (Text-fig. 11D). The structures of the trabecular bone vary in size, from thinner trabeculae of about 40 µm to larger ones reaching even more than 200 µm.

### CONCLUDING REMARKS

Based on the microscopic observations and the histological description of the osteoderms, it appears unlikely that the armour had a thermoregulatory function in contrast to temnospondyl amphibians, for example (Seidel 1979; Grigg and Seebacher 2001; Witzmann *et al.* 2010; Antczak and Bodzioch 2018) or extant crocodylians (Clarac and Quilhac 2019; Handy *et al.* 2019). Dermal sculpture in pseudosuchians is formed by resorption and redeposition – pit excavation with ridges being remnants of the original surface of the bones (Buffrénil 1982; Cerda and

Desojo 2011; Buffrénil *et al.* 2014; Clarac *et al.* 2015; Cerda *et al.* 2018). This allows for a high reduction of the mass of the bones while maintaining their strength (Rinehart and Lucas 2013; Antczak 2016b). Although ornamentation increases the surface of the bone (Rinehart and Lucas 2013), the elements of the armour seem to be very weakly vascularized to effectively help regulate the animal's body temperature or to serve acidosis buffering. Such a role is suggested for dermal bones and osteoderms of early tetrapods or semi-aquatic pseudosuchians, where the vascular networks in dermal bones ornamentation are denser than in the overlying dermis (Janis *et al.* 2012; Clarac *et al.* 2018). The hypothesis about the integration of the bone and dermis is also unlikely. The dermal armour of *S. olenkae* was probably not covered by skin, as there are no thick Sharpey's fibres visible in the external cortex. The osteoderm could be superimposed by epidermal keratinous scales, as is the case with extant crocodylians (Vickaryous and Hall 2008) or turtles (Scheyer 2007). Osteoderms of *Stagonolepis*, that is, of a fully terrestrial animal with poor vascularization, might help to minimise the loss of water in the arid environment of subtropical Pangea, as described for some anuran skull sculpture (Seibert *et al.* 1974). Co-ossification of dermal bones with integument or the covering of the external body surface with bone reduce water loss through skin (Witzmann *et al.* 2010).

More importantly, the collagen fibre organisation of lamellar bone forming the trabeculae of the cancellous core and the layers of the external cortex provides considerable mechanical resistance (Weiner *et al.* 1999; Keaveny *et al.* 2004; Razi *et al.* 2020). The combination of the dense compact layers and porous core of the diploe forms the durable yet lightweight structure of the osteoderms (as was found i.e., for the glyptodont *Glyptotherium arizonae* Gidley, 1926 according to Plessis *et al.* 2018 or in turtle shell as characterised by Scheyer 2007). In addition, numerous bundles of collagen (Sharpey's) fibres in the internal cortex and cancellous core (although not as dense as the structural fibres described by Scheyer and Sander 2004 in ankylosaur osteoderms) could further strengthen the structure of the dermal armour (Scheyer 2007).

Mechanical resistance in some parts of the armour could also be enhanced by particular elements of osteoderm osteology. Clarac *et al.* (2019) found that osteoderms possessing eminences in the form of a dorsal keel reduced stress more efficiently in the case of an attack in a vertical trajectory than osteoderms lacking such structures. The dorsal osteoderms of

the aetosaur *Stagonolepis olenkae* (paramedian and lateral elements) display such eminences – they seem to have been adapted to withstand this type of attack. Ventral and appendicular armour does not have such prominent eminences and is less vulnerable to direct attacks. Clarac *et al.* (2019) examined also the influence of the ornamentation of the osteoderms of selected representatives of Pseudosuchia (including the aetosaur *Aetosaurus* sp.). According to Clarac *et al.* (2019), the ornamentation is supposed to reduce the resistance of the armour elements, but their study treats the osteoderms as a uniform structure, without modelling its diploe structure or taking into consideration the durability of the individual bone-building tissues. The osteoderm of *Aetosaurus* sp. examined by Clarac *et al.* (2019) is characterised by the highest stress endured due to an external attack of all the osteoderms studied. It is also much thinner than the armour elements of *Stagonolepis olenkae*. Therefore, the published results cannot be applied to other members of the Aetosauria clade.

We suggest further experimental stress testing, supported by 3D modelling and simulations of the forces acting on the armour during a hypothetical predator attack, which could provide greater certainty regarding the armour's function.

Additionally, the presence of Sharpey's fibres in the thin section of the lateral osteoderm could represent the remains of collagen fibres originating from the surrounding dermis and incorporated into the developing bone (as indicated in Sharpey's fibre bone by Vickaryous and Hall 2006). Although these fibres are dermal in nature, their formation does not seem to have a metaplastic origin. Unlike the structural fibres (Scheyer and Sander 2004), the dense bundles observed in the lateral osteoderm of *S. olenkae* are completely absent in the secondary bone tissue. Structural fibres have been traced in aetosaur osteoderms several times (Scheyer *et al.* 2014; Cerda *et al.* 2018), but the *S. olenkae* osteoderms analysed seem to lack any potential signs of metaplasia, e.g., possibly due to bone remodelling.

The growth pattern of the UOBS02258 osteoderm differs from the typical annuli-zone sequence (with thick fast-growth zones separated by thin zones of slowed growth – Francillon-Vieillot *et al.* 1990). The observed growth marks reveal a gradual increase in the thickness of both skeletochronological structures towards the outer cortex, but each consecutive annuli is thicker than its corresponding zone. Such a growth pattern is not uncommon for the Late Triassic fauna from Krasiejów. In their study, Teschner *et al.* (2022) focused on the histology of selected *S. olenkae*

humeri. Several growth cycles are characterised by annuli thicker than the preceding zones; lines of arrested growth (LAGs) are also absent, and subsequent cycles can be separated by sporadic rest lines. According to the authors, the unusual growth pattern could be influenced by the relatively moderate climate of Late Triassic Krasiejów, without extreme fluctuations between the wet and dry seasons, corresponding to the climatic conditions proposed by other researchers (e.g., Jewuła *et al.* 2019).

## Acknowledgements

We would like to especially thank Dr. Elżbieta Teschner (Institute of Biology, University of Opole) and Prof. Torsten Scheyer (Department of Paleontology, University of Zürich) for their expertise and helpful advice regarding histological descriptions. We would also like to thank Dr. Tomasz Szczygielski (Institute of Paleobiology, Polish Academy of Science) for his constructive criticism and valuable comments that greatly improved the earlier versions of the manuscript. We wish to thank Szymon Górnicki for providing us with the reconstruction of *Stagonolepis* and Michał Jankowiak for preparing the thin sections. Finally, we are also deeply grateful for the valuable suggestions and feedback from the reviewers.

## REFERENCES

- Agassiz, L. 1844. Monographie des Poissons fossiles du vieux grès rouge ou Système Dévonien (Old Red Sandstone) des Isles Britanniques et de Russie, 171 pp. Jent et Gassman; Neuchâtel.
- Antczak, M. 2012. Jaw osteology and palaeoecology of an aetosaur from the 'Trias' site at Krasiejów, southwest Poland. Budowa osteologiczna czaszki aetozaura ze stanowiska dokumentacyjnego 'Trias' w Krasiejowie. In: Jagt-Yazykova, E., Jagt, J.W.M., Bodzioch, A. and Konietzko-Mejer, D. (Eds), *Krasiejów – palaeontological inspiration*, 55–67. Zakład Poligraficzno-Wydawniczy 'Plik'; Bytom.
- Antczak, M. 2016a. Late Triassic aetosaur (Archosauria) from Krasiejów (SW Poland): new species or an example of individual variation? *Geological Journal*, **51** (5), 779–788.
- Antczak, M. 2016b. Ornamentation of the dermal bones of Placodermi from Devonian deposits of Morocco and increase of mechanical strength. In: Panfil, M. (Ed.), *Badania i Rozwój Młodych Naukowców w Polsce – Weterynaria i botanika*, 61–65. Wydawnictwo Młodzi Naukowcy; Poznań. [In Polish]
- Antczak, M. and Bodzioch, A. 2018. Ornamentation of dermal bones of *Metoposaurus krasiejowensis* and its ecological implications. *PeerJ*, **6**, e5267.

- Bodzioch, A. 2015. Idealized model of mineral infillings in bones of fossil freshwater animals, on the Example of Late Triassic *Metoposaurs* from Krasiejów (Poland). *Austin Journal of Earth Sciences*, **2**, 1008.
- Bodzioch, A. and Kowal-Linka, M. 2012. Unravelling the origin of the Late Triassic multitaxic bone accumulation at Krasiejów (S Poland) by diagenetic analysis. *Palaeogeography, Palaeoclimatology, Palaeoecology*, **346–347**, 25–36.
- Bodzioch, A., Jewuła, K., Matysik, M. and Szulc, J. 2018. Sesja terenowa B. Paleosrodowiskowe uwarunkowania powstawania kopalnych biocenoz i interpretacja procesow tafonomicznych w osadach gornego triasu Slaska. In: Kędzierski, M. and Gradziński, M. (Eds), *Polska Konferencja Sedymologiczna POKOS 7, Góra Św. Anny, 4–7 czerwca 2018 r. Materiały konferencyjne*, 27–32. Polskie Towarzystwo Geologiczne; Kraków.
- Broeckhoven, C., Diedricks, G., le Fras, N. and Mouton, P. 2015. What doesn't kill you might make you stronger: functional basis for variation in body armour. *Journal of Animal Ecology*, **84** (5), 1213–1221.
- Broeckhoven, C., Plessis, A. du and Hui, C. 2017. Functional trade-off between strength and thermal capacity of dermal armor: Insights from girdled lizards. *Journal of the Mechanical Behavior of Biomedical Materials*, **74**, 189–194.
- Buffrénil, V. de 1982. Morphogenesis of bone ornamentation in extant and extinct crocodylians. *Zoomorphology*, **99** (2), 155–166.
- Buffrénil, V. de, Clarac, F., Fau, M., Martin, S., Martin, B., Pellé, E. and Laurin, M. 2014. Differentiation and growth of bone ornamentation in vertebrates: A comparative histological study among the Crocodylomorpha. *Journal of Morphology*, **276**, 425–445.
- Brusatte, S.L., Butler, R.J., Sulej, T. and Niedzwiedzki, G. 2009. The taxonomy and anatomy of rauisuchian archosaurs from the Late Triassic of Germany and Poland. *Acta Palaeontologica Polonica*, **54**, 221–230.
- Casamiquela, R.M. 1960. Noticia preliminar sobre dos nuevos estagonolepoideos Argentinos. *Ameghiniana*, **2**, 3–9.
- Cerda, I.A. and Desojo, J.B. 2011. Dermal armour histology of aetosaurs (Archosauria: Pseudosuchia), from the Upper Triassic of Argentina and Brazil. *Lethaia*, **44**, 417–428.
- Cerda, I.A., Desojo, J.B. and Scheyer, T.M. 2018. Novel data on aetosaur (Archosauria, Pseudosuchia) osteoderm microanatomy and histology: palaeobiological implications. *Palaeontology*, **61**, 721–745.
- Chinsamy, A. and Raath, M.A. 1992. Preparation of fossil bone for histological examination. *Paleontologica africana*, **29**, 39–44.
- Clarac, F., Buffrénil, V. de, Cubo, J. and Quilhac, A. 2018. Vascularization in ornamented osteoderms: physiological implications in ectothermy and amphibious lifestyle in the crocodylomorphs? *The Anatomical Record*, **301** (1), 175–183.
- Clarac, F., Goussard, F., Buffrénil, V. de and Sansalone, V. 2019. The function(s) of bone ornamentation in the crocodylomorph osteoderms: a biomechanical model based on a finite element analysis. *Paleobiology*, **45** (1), 182–200.
- Clarac, F. and Quilhac, A. 2019. The crocodylian skull and osteoderms: A functional exaptation to ectothermy? *Zoology*, **132**, 31–40.
- Clarac, F., Souter, T., Cornette, R., Cubo, J. and Buffrénil, V. de 2015. A quantitative assessment of bone area increase due to ornamentation in the Crocodylia. *Journal of Morphology*, **276**, 1183–1192.
- Dacke, C.G., Elsey, R.M., Trosclair III, P.L., Sugiyama, T., Nevarez, J.G. and Schweitzer, M.H. 2015. Alligator osteoderms as a source of labile calcium for eggshell formation. *Journal of Zoology*, **297** (4), 255–264.
- Desojo, J.B., Heckert, A.B., Martz, J.W., Parker, W.G., Schoch, R.R., Small, B.J. and Sulej, T. 2013. Aetosauria: a clade of armoured pseudosuchians from the Upper Triassic continental beds. *Geological Society, London, Special Publications*, **379**, 203–239.
- Desojo, J.B. and Vizcaino, S.F. 2009. Jaw biomechanics in the South American aetosaur *Neoaetosauroides engaeus*. *Paläontologische Zeitschrift*, **83**, 499–510.
- Drózd, D. 2018. Osteology of a forelimb of an aetosaur *Stagonolepis olenkae* (Archosauria: Pseudosuchia: Aetosauria) from the Krasiejów locality in Poland and its probable adaptations for a scratch-digging behavior. *PeerJ*, **6**, e5595.
- Drymala, S.M., Bader, K. and Parker, W.G. 2021. Bite marks on an aetosaur (Archosauria, Suchia) osteoderm: assessing Late Triassic Predator-prey ecology through ichnology and tooth morphology. *Palaios*, **36**, 28–37.
- Dzik, J. 2003. A beaked herbivorous archosaur with dinosaur affinities from the early Late Triassic of Poland. *Journal of Vertebrate Paleontology*, **23**, 556–574.
- Dzik, J. and Sulej, T. 2007. A review of the early Late Triassic Krasiejów biota from Silesia, Poland. *Palaeontologica Polonica*, **64**, 3–27.
- Dzik, J., Sulej, T., Kaim, A. and Niedzwiedzki, R. 2000. A late Triassic tetrapod graveyard in the Opole Silesia (SW Poland). *Przegląd Geologiczny*, **48**, 226–235. [In Polish]
- Fijałkowska-Mader, A. 2015. Record of climatic changes in the Triassic palynological spectra from Poland. *Geological Quarterly*, **59**, 615–653.
- Fraas, E. 1889. Die Labyrinthodonten aus der Schwäbischen Trias. *Palaeontographica*, **36**, 1–158.
- Francillon-Vieillot, H., Buffrénil, V. de, Castanet, J., Géraudie, J., Meunier, F.J., Sire, J.Y., Zylberberg, L. and Ricqlès, A. de. 1990. Microstructure and mineralization of vertebrate skeletal tissues. In: Carter, J.G. (Ed), *Skeletal biomineralization: patterns, processes and evolutionary trends*, 1, 471–530. Van Nostrand Reinhold; New York.
- Grigg, G. and Seebacher, F. 2001. Crocodylian thermal relations. In: Grigg, G., Seebacher, F. and Franklin, C.E. (Eds),

- Crocodylian Biology and Evolution, 297–309. Surrey Beaty & Sons; Chipping Norton.
- Gruszka, B. and Zieliński, T. 2008. Evidence for a very low-energy fluvial system: A case study from the dinosaur-bearing Upper Triassic rocks of Southern Poland. *Geological Quarterly*, **52**, 239–252.
- Handy, S., Ceja, M. and Arnette, J. 2019. The potential role of osteoderms during thermoregulation in the American alligator. *OSR Journal of Student Research*, **5**, 264.
- Heckert, A.B., Fraser, N.C. and Schneider, V.P. 2017. A new species of *Coahomasuchus* (Archosauria, Aetosauria) from the Upper Triassic Pekin Formation, Deep River Basin, North Carolina. *Journal of Paleontology*, **91**, 162–178.
- Heckert, A.B. and Lucas, S.G. 1999. A new aetosaur (Reptilia: Archosauria) from the Upper Triassic of Texas and the phylogeny of aetosaurs. *Journal of Vertebrate Paleontology*, **19** (1), 50–68.
- Heckert, A.B. and Lucas, S.G. 2000. Taxonomy, phylogeny, biostratigraphy, biochronology, paleobiogeography, and evolution of the Late Triassic Aetosauria (Archosauria: Crurotarsi). *Zentralblatt für Geologie und Paläontologie, Teil I*, **1998** (11–12), 1539–1587.
- Hoffman, D.K., Heckert, A.B. and Zanno, L.E. 2018. Disparate growth strategies within Aetosauria: Novel Histologic Data from the aetosaur *Coahomasuchus chathamensis*. *The Anatomical Record*, **302** (9), 1504–1515.
- Houssaye, A. 2009. “Pachyostosis” in aquatic amniotes: a review. *Integrative Zoology*, **4**, 325–340.
- Janis, C.M., Devlin, K., Warren, D.E. and Witzmann, F. 2012. Dermal bone in early tetrapods: a paleophysiological hypothesis of adaptation for terrestrial acidosis. *Proceedings of the Royal Society B—Biological Sciences*, **279**, 3035–3040.
- Jewuła, K., Matysik, M., Paszkowski, M. and Szulc, J. 2019. The late Triassic development of playa, gilgai floodplain, and fluvial environments from Upper Silesia, southern Poland. *Sedimentary Geology*, **379**, 25–45.
- Keaveny, T.M., Morgan, E.F. and Yeh, O.C. 2004. Bone mechanics. In: Myer, K. (Ed.), *Standard handbook of biomedical engineering and design*, 8.1–8.23. McGraw-Hill; New York.
- Keeble, E. and Benton, M.J. 2020. Three-dimensional tomographic study of dermal armour from the tail of the Triassic aetosaur *Stagonolepis robertsoni*. *Scottish Journal of Geology*, **56**, 55–62.
- Konieczna, N., Belka, Z. and Dopieralska, J. 2015. Nd and Sr isotopic evidence for provenance of clastic material of the Upper Triassic rocks of Silesia, Poland. *Annales Societatis Geologorum Poloniae*, **85**, 675–684.
- Kowalski, J., Bodzioch, A., Janecki, P.A., Ruciński, M.R. and Antczak, M. 2019. Preliminary report on the microvertebrate faunal remains from the Late Triassic locality at Krasiejów, SW Poland. *Annales Societatis Geologorum Poloniae*, **89**, 291–305.
- Lucas, S.G. 2015. Age and correlation of Late Triassic tetrapods from southern Poland. *Annales Societatis Geologorum Poloniae*, **85**, 627–635.
- Lucas, S.G. 2020. Biochronology of Late Triassic Metoposauridae (Amphibia, Temnospondyli) and the Carnian pluvial episode. *Annales Societatis Geologorum Poloniae*, **90**, 409–418.
- Lucas, S.G., Spielmann, J.A. and Hunt, A.P. 2007. Biochronological significance of Late Triassic tetrapods from Krasiejów, Poland. *New Mexico Museum of Natural History and Science Bulletin*, **41**, 248–258.
- Lydekker, R. 1885. The Reptilia and Amphibia of the Maleri and Denwa groups. *Palaeontologia Indica, Series I*, **1**, 1–38.
- Lydekker, R. 1890. Catalogue of the fossil Reptilia and Amphibia in the British Museum of Natural History. Part IV, 295 pp. British Museum of Natural History; London.
- Mitchell, J. and Sander, P.M. 2014. The three-front model: a developmental explanation of long bone diaphyseal histology of Sauropoda. *Biological Journal of the Linnean Society*, **112**, 765–781.
- Nasoori, A. 2020. Formation, structure, and function of extra-skeletal bones in mammals. *Biological Reviews*, **95** (4), 986–1019.
- Nesbitt, S.J. 2011. The early evolution of archosaurs: relationships and the origin of major clades. *Bulletin of the American Museum of Natural History*, **352**, 1–292.
- Parker, W.G. 2003. Description of a new specimen of *Desmatosuchus haplocerus* from the Late Triassic of Northern Arizona. Unpublished M.Sc. thesis, Northern Arizona University, 315 pp. Flagstaff, Arizona.
- Parker, W.G. 2016. Osteology of the Late Triassic aetosaur *Scutarx deltatylus* (Archosauria: Pseudosuchia). *PeerJ*, **4**, e2411.
- Parker, W.G. 2018. Anatomical notes and discussion of the first described aetosaur *Stagonolepis robertsoni* (Archosauria: Suchia) from the Upper Triassic of Europe, and the use of plesiomorphies in aetosaur biochronology. *PeerJ*, **6**, e5455.
- Plessis, A. du, Broeckhoven, C., Yadroitsev, I., Yadroitsava, I. and le Roux, S.G. 2018. Analyzing nature’s protective design: The glyptodont body armor. *Journal of the Mechanical Behavior of Biomedical Materials*, **82**, 218–223.
- Pochat-Cottilloux, Y., Martin, J.E., Amiot, R., Cubo, J. and Buffrénil, V. de 2022. A survey of osteoderm histology and ornamentation among Crocodylomorpha: A new proxy to infer lifestyle? *Journal of Morphology*, **284** (1), 374–393.
- Razi, H., Predan, J., Fischer, F.D., Kolednik, O. and Fratzl, P. 2020. Damage tolerance of lamellar bone. *Bone*, **130**, 115102.
- Rinehart, L.F. and Lucas, S.G. 2013. The functional morphology of dermal bone ornamentation in temnospondyl amphibians. In: Tanner, L.H., Spielmann, J.A. and Lucas, S.G. (Eds), *The Triassic system. New Mexico Museum of Natural History and Science Bulletin*, **61**, 524–532.

- Robling, A.G. and Stout, S.D. 1999. Morphology of the drifting osteon. *Cells Tissues Organs*, **164**, 192–204.
- Scheyer, T.M. 2007. Comparative bone histology of the turtle shell (carapace and plastron): implications for turtle systematics, functional morphology and turtle origins. Unpublished PhD Thesis, 343 pp. University of Bonn.
- Scheyer, T.M., Desojo, J.B. and Cerda, I.A. 2014. Bone histology of phytosaur, aetosaur, and other archosauriform osteoderms (Eureptilia, Archosauromorpha). *The Anatomical Record Advances in Integrative Anatomy and Evolutionary Biology*, **297** (2), 240–260.
- Scheyer, T.M. and Sander, P.M. 2004. Histology of ankylosaur osteoderms: implications for systematics and function. *Journal of Vertebrate Paleontology*, **24** (4), 874–893.
- Seibert, E.A., Lillywhite, H.B. and Wassersug, R.J. 1974. Cranial co-ossification in frogs: relationship to rate of evaporite water loss. *Physiological Zoology*, **47**, 261–265.
- Seidel, M.R. 1979. The osteoderms of the American *Alligator* and their functional significance. *Herpetologica*, **35**, 375–380.
- Small, B.J. 1985. The Triassic Thecodontian Reptile *Desmatosuchus*: Osteology and Relationships. Unpublished MSc. Thesis, Texas Technical University, 83 pp. Lubbock.
- Small, B.J. 2002. Cranial anatomy of *Desmatosuchus haplocerus* (Reptilia: Archosauria: Stagonolepididae). *Zoological Journal of the Linnean Society*, **136**, 97–111.
- Sulej, T. 2005. A new rauisuchian reptile (Diapsida: Archosauria) from the Late Triassic of Poland. *Journal of Vertebrate Paleontology*, **25**, 75–83.
- Sulej, T. 2010. The skull of an early Late Triassic aetosaur and the evolution of the stagonolepidid archosaurian reptiles. *Zoological Journal of the Linnean Society*, **158**, 860–881.
- Sulej, T. and Majer, D. 2005. The temnospondyl amphibian *Cyclotosaurus* from the Upper Triassic of Poland. *Palaeontology*, **48**, 157–170.
- Szulec, J. 2005. Sedimentary environments of the vertebrate-bearing Norian deposits from Krasiejów, Upper Silesia (Poland). *Hallesches Jarbuch für geowissenschaften Reihe B*, **19**, 161–170.
- Szulec, J. and Racki, G. 2015. Grabowa Formation – the basic lithostratigraphic unit of the Upper Silesian Keuper. *Przełąd Geologiczny*, **63**, 103–113. [In Polish]
- Szulec, J., Racki, G. and Jewuła, K. 2015a. Key aspects of the stratigraphy of the Upper Silesian middle Keuper, southern Poland. *Annales Societatis Geologorum Poloniae*, **85**, 557–586.
- Szulec, J., Racki, G., Jewuła, K. and Środoń, J. 2015b. How many Upper Triassic bone-bearing levels are there in Upper Silesia (southern Poland)? A critical overview of stratigraphy and facies. *Annales Societatis Geologorum Poloniae*, **85**, 587–626.
- Środoń, J., Szulec, J., Anczkiewicz, A., Jewuła, K., Banaś, M. and Marynowski, L. 2014. Weathering, sedimentary, and diagenetic controls of mineral and geochemical characteristics of the vertebrate-bearing Silesian Keuper. *Clay Minerals*, **49**, 569–594.
- Taborda, J.R.A., Desojo, J.B. and Dvorkin, E.N. 2021. Biomechanical skull study of the aetosaur *Neoaetosauroides engaeus* using Finite Element Analysis. *Ameghiniana*, **58** (5), 401–415.
- Teschner, E.M., Konietzko-Meier, D. and Klein, N. 2022. Growth and limb bone histology of aetosaurs and phytosaurs from the Late Triassic Krasiejów locality (SW Poland) reveals strong environmental influence on growth pattern. *Contributions to Zoology*, **91** (3), 199–232.
- Vickaryous, M.K. and Hall, B.K. 2008. Development of the dermal skeleton in *Alligator mississippiensis* (Archosauria, Crocodylia) with comments on the homology of osteoderms. *Journal of Morphology*, **269**, 398–422.
- Witzmann, F., Scholz, H., Müller, J. and Kardjilov, N. 2010. Sculpture and vascularization of dermal bones and the implications for the physiology of basal tetrapods. *Zoological Journal of the Linnean Society*, **160**, 302–340.
- Weiner, S., Traub, W. and Wagner, H.D. 1999. Lamellar Bone: Structure–Function Relations. *Journal of Structural Biology*, **126** (3), 241–255.
- Zittel, K.A. 1887. Handbuch der Palaeontologie. Abteilung Palaeozoologie, 900 pp. R. Oldenbourg; Munich and Leipzig.

Manuscript submitted: 21<sup>st</sup> June 2024

Revised version accepted: 18<sup>th</sup> November 2024